

1 **Comparative evaluation of continuous piggery wastewater treatment**
2 **in open and closed purple phototrophic bacteria-based**
3 **photobioreactors.**

4
5 Cristian A. Sepúlveda-Muñoz ^{a, b}, Roxana Ángeles ^{a, b}, Ignacio de Godos ^{b, c}, Raúl
6 Muñoz ^{a, b, *}

7
8 ^a Department of Chemical Engineering and Environmental Technology, School of
9 Industrial Engineering, University of Valladolid, Dr. Mergelina, s/n, 47011 Valladolid,
10 Spain.

11 ^b Institute of Sustainable Processes, Dr. Mergelina, s/n, 47011 Valladolid, Spain.

12 ^c School of Forestry, Agronomic and Bioenergy Industry Engineering (EIFAB),
13 University of Valladolid, Campus Duques de Soria, 42004, Soria, Spain.

14
15 * Corresponding author: e-mail mutora@iq.uva.es (R. Muñoz)

16
17
18
19
20
21
22
23

24 **Abstract**

25 Purple phototrophic bacteria (PPB) represent an innovative approach for wastewater
26 treatment with a high metabolic plasticity, able to grow under aerobic and anaerobic
27 conditions. This study comparatively assessed the long-term performance (450 days of
28 operation) of an open and closed PPB-based photobioreactor treating of piggery
29 wastewater (PWW). The influence of wastewater dilution, illuminated area to volume
30 ratio, biomass settling and recirculation, and infrared light intensity on wastewater
31 treatment was evaluated at 7 days of hydraulic retention time. An increase in PWW
32 dilution from 4 to 8 folds did not entail higher TOC removal efficiencies (REs) in the
33 open photobioreactor (87% versus 89%), but a significant increase in the closed
34 photobioreactor (from 73% to 80%). The increase in the illuminated area to volume ratio
35 increased TN-REs up to 99% and 49% in the open and closed photobioreactor,
36 respectively, with a concomitant increase in the temperature of both systems. However,
37 temperature control did not mediate a significant enhancement in PWW treatment.
38 Biomass settling and recirculation resulted in higher TN-REs (80%) and TOC-REs (90%)
39 in the closed photobioreactor. The increase in infrared radiation from 100 to 300 W m⁻²
40 fostered PPB growth. High water evaporation losses (deteriorating effluent quality) were
41 recorded in the open photobioreactor, where carbon dioxide and ammonia stripping were
42 identified as the main pathways supporting carbon and nitrogen removal.

43

44 **Keywords:** Nutrient removal; PPB; Purple non-sulphur bacteria; Photosynthetic bacteria;
45 Swine manure.

46

47

48

49 **1. Introduction**

50 High strength wastewaters such as those produced by intensive animal husbandry
51 represent a severe environmental problem that is also limiting the growth of this economic
52 sector in Europe. Piggery wastewater (PWW) is characterized by a high content of
53 particulate and dissolved organic carbon, nitrogen (mainly in the form of NH_4^+) and
54 phosphorous due to the limited use of water during farming [1–3], which can severely
55 damage water bodies and soil if not properly managed [4]. In this context, photosynthetic
56 microorganisms have been proposed as cost-effective platforms for the removal of
57 nutrients and carbon from PWW [3,5–9]. Photosynthetic microorganisms represent
58 unique microbial cell factories due to their ability to fix carbon and nutrients using energy
59 from solar light, via oxygenic and anoxygenic photosynthesis in the case of microalgae
60 and purple phototrophic bacteria (PPB), respectively [10,11].

61

62 PPB exhibit a superior metabolism compared to other photosynthetic microorganisms
63 (microalgae and green sulfur bacteria), which is characterized by high growth rates [12],
64 tolerance to low temperatures [13], and ability to assimilate multiple substrates and grow
65 in any kind of wastewater [14]. PPB are among the most metabolically versatile
66 microorganisms that can grow under chemotrophic, phototrophic and mixotrophic
67 condition. Under aerobic chemotrophic metabolism, pollutant bio-degradation occurs
68 mainly by oxidative phosphorylation [15]. However, the competition with aerobic
69 chemoheterotrophic bacteria in aerated tank treating wastewater decreases the
70 concentration of PPB [16], whose metabolism is favored at low oxygen concentrations.
71 On the other hand, PPB are able to grow phototrophically using near infrared light energy
72 as energy source under anaerobic conditions [17]. PPB can fix CO_2 via the Calvin-
73 Benson-Bassham pathway, and encode the Embden-Meyerhof pathway, tricarboxylic

74 acid cycle (TCA), pentose phosphate and multiple aromatic biodegradation pathways
75 [17]. In addition, PPBs can assimilate all forms of nitrogen (including N₂), which supports
76 their high potential for the assimilation of nutrients from wastewater [14]. Finally, PPB
77 biomass is rich in value-added products such single cell protein, pigments (carotenoids
78 and bacteriochlorophylls), biopolymers (PHA), antimicrobial agents, pantothenic acid,
79 coenzyme Q10 and amino acid 5-ALA [11,18,19].

80

81 The photo-anaerobic membrane bioreactor has been the main configuration used for the
82 treatment of domestic, dairy, food and poultry processing wastewater with PPB [10,20–
83 22]. However, despite their efficiency [23], the use of membranes hinders the industrial
84 scale up of this bioreactor configuration due to the need for complex control systems and
85 the increase in operating costs [24]. In this context, the engineering of simple and cost-
86 effective photobioreactor configurations remains an unresolved challenge for PPB-based
87 treatment PWW. Shallow covered ponds with biomass settling and recycling represent a
88 cost-effective but poorly explored photobioreactor configuration to treat wastewater
89 using PPB. The key operational conditions determining the performance of PPB-ponds
90 with biomass settling and recycling need to be also investigated.

91

92 In this work, the long-term performance of two PPB-based photobioreactor
93 configurations (open and closed) during the treatment of PWW was evaluated. The
94 influence of wastewater dilution, illuminated area to volume ratio, biomass settling and
95 recirculation, and infrared light intensity on the removal of carbon and nitrogen was
96 comparatively assessed.

97

98 **2. Materials and Methods**

99 *2.1. Inoculum and piggery wastewater*

100 The inoculum of PPB was taken from a batch cultivation of a previous study with
101 *Rhodopseudomonas* as the dominant genus [6]. Inoculum of PPB was carried out in 1.2
102 L gas-tight bottles (Afora, Spain) with 600 mL of four times diluted piggery wastewater
103 under a N₂ atmosphere. The PPB culture was incubated at room temperature (25 ± 1 °C)
104 under magnetic mixing (300 rpm) and an infrared lighting (50 W m⁻²). Centrifuged PWW
105 was obtained from a pig farm in Segovia (Spain) and maintained at 4 °C prior use. The
106 PWW was further centrifuged (10,000 rpm, 10 min) prior to use. The characteristics of
107 the PWW used in the experiments was: total organic carbon concentration (TOC) of 9.4
108 ± 1.2 g L⁻¹, total carbon concentration (TC) of 10.5 ± 1.0 g L⁻¹, inorganic carbon
109 concentration (IC) of 1.0 ± 0.3 g L⁻¹, total nitrogen concentration (TN) of 3.0 ± 0.4 g L⁻¹
110 and total suspended solids concentration (TSS) of 10.5 ± 2.2 g L⁻¹.

111

112 *2.2. Continuous PWW biodegradation in open and closed photobioreactors*

113 The experimental set-up consisted of two rectangular photobioreactors (20 cm length ×
114 10 cm width × 15 cm depth; 3 L of working volume) (Fig. 1) constructed with transparent
115 covers and interconnected to 1 L conical settlers. The covers were placed either 2 cm
116 above the top of the open photobioreactor (PBR) to favor air supply or at the cultivation
117 broth surface level in the closed PBR to guarantee anaerobic conditions. The systems
118 were agitated with two submerged centrifugal pumps. The PBRs were illuminated at 100
119 W m⁻² (stages I-V) or 300 W m⁻² (stages VI) for 12 h a day using an infrared LED panel
120 (diodes OSLUX® SFH 4780S and SFH 4715AS, OSRAM, Germany) located 20 cm
121 above the surface of the cultivation broth. The PBRs were initially operated at a hydraulic
122 retention time (HRT) of 7 days using 4 folds diluted PWW (stage I). An aliquot of 56 and
123 12 mL in stage I-II and III-IV respectively, was daily drawn from the bottom of the settler

124 to waste the settled biomass. The dilution of the PWW was increased to 8 fold by day 102
125 and maintained for the rest of the experiment (stage II). In stage III, the illuminated area
126 to volume ratio was increased from 66.7 cm² L⁻¹ to 133 cm² L⁻¹ by reducing the working
127 volume of the PBRs to 1.5 L (via a reduction in the PBR depth from 15 cm to 7.5 cm). A
128 cooling system based on PBR jacketing was implemented in both PBRs by day 239
129 (beginning of stage IV) to maintain similar temperatures as in stage II due to the increase
130 in temperature mediated by the heat generated by the submerged centrifugal pumps in the
131 new working volume. In stage V, biomass recirculation from the bottom of the conical
132 settlers was implemented at a rate of 167 mL d⁻¹. Finally, the intensity of the infrared
133 radiation was increased to 300 W m⁻² during stage VI (Table 1).

134 <Figure 1>

135 <Table 1>

136 Samples of 20 mL from the centrifuged PWW (raw influent), cultivation broth and
137 effluent of the open and closed PBRs were collected systematically twice a week to
138 analyze pH and TOC, TC, IC, TN, NH₄⁺ and TSS concentrations. The dissolved oxygen
139 concentration (DO) and temperature in the culture broths of the PBRs was in-situ
140 measured twice a week. The culture absorbance in the each PBR was also measured twice
141 a week. In addition, an aliquot of biomass from each steady state (10 min at 10,000 rpm)
142 was centrifuged, washed and dried to analyze its elemental composition (C, H, O and N
143 content).

144 The removal efficiencies (REs), expressed in percentage, of TOC, TN and TSS were
145 calculated according to the following equation:

$$146 \quad RE (\%) = \frac{(C_{inf} \cdot Q_{inf}) - (C_{eff} \cdot Q_{eff})}{(C_{inf} \cdot Q_{inf})} \cdot 100$$

147 Where C_{inf} and C_{eff} correspond to the concentration of TOC, TN and TSS in the piggery
148 wastewater influent and effluent of the PBRs, respectively, while Q_{inf} and Q_{eff} correspond

149 to the flowrate in the piggery wastewater influent and effluent of the PBRs, respectively.
150 The removal efficiencies were calculated in steady state for each PBR.

151

152 *2.3. Analytical methods*

153 The pH determinations were conducted with a pH 510 pHmeter (Cyberscan,
154 Netherlands). A ProfiLine 3320 meter coupled with a sensor CellOx 325 (WTW,
155 Germany) was used to measure the DO and temperature. Infrared light intensity was
156 determined with a PASPort PS-2148 IR sensor (PASCO, USA). Measurements of
157 dissolved TOC, TC, IC and TN concentrations were carried out in a TOC-VCSH
158 instrument (Shimadzu, Japan) coupled with a TNM-1 unit. The spectrum of absorbance
159 (350–850 nm) of the cultivation broth was analyzed in a spectrophotometer UV-2550
160 (Shimadzu, Japan). NH_4^+ analysis was conducted using a sensor Orion Dual Star
161 (ThermoScientific, The Netherlands). The elemental composition was analyzed using an
162 elemental analyzer EA Flash 2000 equipped with a TCD detector (Thermo Fisher
163 Scientific). Finally, the quantification of TSS concentration was performed following the
164 procedure of Standard Methods [25].

165

166 *2.4. Statistical analysis*

167 Statgraphics Centurion version 18 was used for the analysis of variance (ANOVA) and a
168 Tukey test carried out to identify the significance of the values obtained, comparisons
169 with a value of $p < 0.05$ were considered significant. Performed to the experimental data
170 obtained under steady state.

171

172 **3. Results and Discussion**

173 *3.1. Environmental parameters*

174 Temperatures in the closed PBR were higher than those in the open PBR as a result of the
175 evaporation-based heat losses in the latter, with average values of 32 ± 1 °C and 36 ± 2
176 °C in the open and closed PBR, respectively. Temperatures of 32 ± 1 °C and 35 ± 3 °C in
177 stage I, and 31 ± 1 °C and 33 ± 1 °C in stage II, were recorded in the open and closed
178 PBR, respectively (Table 2). The heat generated by the submerged mixing pumps resulted
179 in a high increase in temperatures in the closed PBR in stage III, where temperatures
180 reached 40 °C occasionally due to the low PBR volumes compared to stage I and II (Fig.
181 S1A). Likewise, an increase in temperature was recorded in stage VI in both PBRs ($34 \pm$
182 0 °C in open the PBR and 40 ± 2 °C in the closed PBR) due to the increase in IR radiation.
183 The optimal growth temperature in biological wastewater treatment is species specific.
184 For instance, *Rhodopseudomonas palustris* exhibits optimum growth at 37 °C, while *R.*
185 *capsulatus* and *R. spheroids* growth rate peaks at 30 °C [26]. Although the temperatures
186 recorded in this work were high, the communities present in both PBRs were able to adapt
187 and support an efficient removal of carbon and nutrients as described below. These high
188 temperatures prevailing in the cultivation broth mediated the high evaporation rates
189 observed in the open PBR, which accounted for 58, 97, 84, 89 and 99% of the inlet flow
190 in stages I-II, III, IV, V and VI, respectively. This resulted in low effluent flowrates in
191 the stages with higher temperature (stage III and VI). The loss of water in open ponds
192 devoted to photosynthetic microorganisms cultivation due to evaporation entails higher
193 operational costs (due to the need for water make-up), and can also increase the risk of
194 contamination with unwanted microorganisms [27]. In addition, the high evaporation rate
195 herein recorded in the open PBR resulted in the concentration of the effluent pollutants,
196 thus impacting on the removal efficiencies of the open PBR [6]. On the other hand,
197 although the temperatures recorded in the closed PBR were higher than in the open PBR,
198 the evaporation rates averaged of 10, 30, 14, 17 and 11% in stages I-II, III, IV, V and VI,

199 respectively, and likely occurred in the open settler interconnected to the PBR. This PBR
200 configuration favors the recovery of treated water, which is central in areas with severe
201 water stress such as the Mediterranean region.

202 <Table 2>

203 The dissolved oxygen (DO) concentration remained very low in both PBRs regardless of
204 the operational conditions (Fig. S1B), with average values of 0.03 ± 0.01 and 0.02 ± 0.01
205 $\text{mg O}_2 \text{ L}^{-1}$ in the open and closed PBR, respectively. The oxygen diffusing from the open
206 atmosphere into the open PBR cultivation broth was rapidly consumed by
207 chemoheterotrophic PPB or other aerobic heterotrophic bacteria for the degradation of
208 organic matter. The low oxygen concentration in the closed PBR, caused by the negligible
209 oxygen input into this system and the high organic matter content of the PWW,
210 maintained strict anaerobic conditions in the cultivation broth. In this context, low
211 dissolved oxygen concentration ($\text{DO} < 0.5 \text{ mg L}^{-1}$ which is considerable higher than the
212 values detected in both reactors) promote the activity of the enzyme dehydrogenase [28],
213 which favors the degradation of organic compounds through the TCA cycle in PPB.
214 According to previous studies, aerobic conditions during wastewater treatment limit the
215 development of PPB [16].

216 The pH of the PWW was 7.8 ± 0.3 , while the pH of the cultivation broths remained very
217 stable along the different stages tested (Fig. S1C), with pH values of 8.7 ± 0.1 and $8.3 \pm$
218 0.2 in the open and closed PBRs, respectively. The higher pH in the open PBR was likely
219 due to the stripping of CO_2 from the cultivation broth to the open atmosphere. Likewise,
220 the degradation of volatile fatty acids (VFAs) by PPB likely induced the increase in pH
221 observed in both PBRs due to the consumption of organic acids by VFAs catabolic
222 pathways, which also enhanced the fixation of the dissolved CO_2 [12]. The optimal pH
223 range described for PPB is 6.0 to 9.0 [14], which matched the pH recorded in both PBRs.

224

225 3.2. Wastewater treatment performance

226 3.2.1. Carbon removal

227 The TOC concentration in the influent (PWW) was maintained constant in stage I at 2.7
228 $\pm 0.2 \text{ g L}^{-1}$ TOC and $1.2 \pm 0.1 \text{ g L}^{-1}$ in the following stages (II-VI) (Fig. 2A). High carbon
229 removal efficiencies of $87 \pm 1\%$ and $73 \pm 2\%$ were recorded under steady state in stage I
230 in the open and closed PBR, respectively (Fig. 3A). However, a limited PPB growth was
231 observed in both PBRs as shown by gradual disappearance of the characteristic purple-
232 red color in the cultivation broths. Independent measurements of infrared light penetration
233 in 4 fold diluted PWW showed that the photic zone was only $\sim 1 \text{ cm}$ due to the high
234 wastewater turbidity. The limited growth of PPB was attributed to the low penetration of
235 IR radiation in both PBRs, which resulted in a reduced capacity of PPBs to obtain energy
236 from anoxygenic photosynthesis and to degrade organic carbon. In this context, PPB in
237 the absence of or under limited infrared light supply are not able to compete with other
238 chemotrophic bacteria as a result of their less efficient fermentative metabolism [16]. An
239 increase in PWW dilution resulted in a significant increase in TOC-REs in stage II up to
240 $89 \pm 1\%$ and $80 \pm 2\%$ in the open and closed PBR, respectively. The increase in PWW
241 dilution enhanced the penetration of IR radiation, doubling the photic zone depth and thus
242 favoring the growth of PPB and the removal of carbon. In this context, the increase in the
243 illuminated area to volume ratio caused by the reduction in the depth of both PBRs from
244 15 to 7.5 cm in stage III significantly favored the removal of carbon, with TOC-REs of
245 $99 \pm 0\%$ and $84 \pm 2\%$ in the open and closed PBR, respectively. This increase in the
246 illuminated area to volume ratio also mediated an increase in the temperature of the
247 cultivation broths and in the water evaporation rates, which suggests that the
248 improvement in TOC removal in the open PBR was not only due to an enhanced PPB

249 activity but also to a higher stripping of carbon dioxide. An environmental benefit derived
250 from the implementation of closed PBRs is the reduction in gas emissions into the
251 atmosphere, which prevents the release of CO₂ and CH₄ potentially generated under
252 anaerobic conditions. Temperature control in stage IV did not favor TOC-REs in the open
253 PBR, which decreased to 91 ± 1%, but increased TOC-REs by 4% in the closed PBR
254 compared to the previous stage (III), likely due to the increase in PPB activity. The
255 recirculation of the settled biomass in stage V resulted in an improvement in TOC-REs
256 up to 96 ± 1% and 90 ± 1% in the open and closed PBRs, respectively. This improvement
257 was likely due to the increase in PPB biomass in the PBRs, which boosted the removal of
258 the carbon present in PWW. Finally, the increase in IR radiation intensity in stage VI
259 from 100 to 300 W m⁻² (Fig. S1D) did not significantly improve the removal of carbon in
260 the closed PBR (TOC-REs of 91 ± 1%), but resulted in a complete TOC removal in the
261 open PBR due to the increase in the evaporation rate. The results herein obtained
262 confirmed the consistent removals of organic matter by PPB and were in agreement with
263 the TOC-REs of 87, 84 and 77% recorded by García et al. (2019) in an open
264 photobioreactor treating PWW at HRTs of 10.6, 7.6 and 4.1 days respectively, using 20
265 fold diluted PWW [6].

266 <Figure 2>

267 <Figure 3>

268 A preliminary carbon mass balance revealed that the closed PBR supported higher carbon
269 recoveries than the open PBR (e.g. 82% vs 52% in stage I). Overall, carbon recovery in
270 the closed PBR was 36% higher than in the open PBR. The main mechanism of carbon
271 removal in the open PBR was stripping, and assimilation in the closed PBR, which agreed
272 with the water evaporation rates recorded in both systems.

273

274 3.2.2. Nitrogen removal

275 In stage I, TN-REs of $78 \pm 1\%$ and $21 \pm 3\%$ were recorded in the open and closed PBR,
276 respectively (Fig. 3B). Similarly, the removal of ammonia was higher in the open PBR
277 (0.58 g L^{-1} removed) compared to that in the closed PBR (0.21 g L^{-1} removed). A slight
278 decrease in TN-REs to $72 \pm 2\%$ and $17 \pm 4\%$ in the open and closed PBR, respectively,
279 was observed in stage II along with the increase in PWW dilution. The high TN removal
280 observed in the open PBR in stages I and II can be explained by the active ammonium
281 stripping from the PBR to the atmosphere [8] and by the consumption of nitrogen by other
282 microorganisms different from PPB. On the other hand, the low TN removal recorded in
283 the closed PBR was attributed mainly to the assimilation of NH_4^+ into biomass (in the
284 form of microbial protein), since the air-tight PBR cover prevented ammonium stripping
285 in this type of configuration. In stage III an increase of TN-REs was recorded with $99 \pm$
286 0% and $49 \pm 6\%$ in the open and closed PBR, respectively, which was likely induced by
287 the higher PPB growth favored by the increased illuminated area to volume ratio in both
288 PBRs. The decrease in temperatures during stage IV resulted in TN-REs of $95 \pm 1\%$ and
289 $43 \pm 7\%$ in the open and closed PBRs, respectively. The effluent obtained during stage
290 IV presented low concentrations of NH_4^+ (0.00 g L^{-1} in the open PBR and 0.17 g L^{-1} in
291 the closed PBR). Interestingly, the implementation of the recirculation of the settled
292 biomass in stage V brought about higher TN-REs of $98 \pm 0\%$ in the open PBR and $80 \pm$
293 4% in the closed PBR. The analysis of the concentrations of ammonium during stage V
294 was not possible due to a failure of the NH_4^+ electrode (Table 2). Finally, the increase in
295 IR radiation during stage VI supported TN-REs and ammonium effluent concentrations
296 of $100 \pm 0\%$ and $0.02 \text{ g NH}_4^+ \text{ L}^{-1}$ in the open PBR, and $79 \pm 2\%$ and $0.08 \text{ g NH}_4^+ \text{ L}^{-1}$ in
297 the closed PBR. Removals efficiencies of 65% for total nitrogen and 68% for ammonium
298 have been reported in an open photobioreactor treating PWW with PPB at a HRT of 7.6

299 days [6]. Ammonia is the main form of nitrogen present in PWW, which can be
300 assimilated by PPB through glutamate metabolism and subsequently used in protein
301 synthesis. This metabolic capacity is present in PPBs species such as *R. palustris*, *R*
302 *capsulatus* and *R. sphaeroides*. During stages V and VI, 0.29 ± 0.02 and 0.27 ± 0.02 g N
303 L^{-1} were removed in the open and closed PBR, respectively (Fig. 2B), which lies within
304 the 3-8000 mg L^{-1} range described in literature studies assessing nitrogen removal by PPB
305 [28]. Nitrogen removal could be improved by increasing the C:N ratio [12] in PWW using
306 C-rich wastewaters to support a complete assimilation of the nitrogen present in PWW.

307

308 3.3. Concentration and elemental composition of biomass

309 Biomass concentration in the open PBR increased during the first 50 days from 1.7 g TSS
310 L^{-1} up to 5.6 g TSS L^{-1} in stage I, along with a rapid disappearance of the purple-red color
311 in the cultivation broth, suggesting an adaptation of other microbial communities.
312 Interestingly, biomass concentration in the open PBR gradually decreased to 3.8 g TSS
313 L^{-1} by the end of stage I likely due to natural cell death or the toxic effects of the
314 accumulated PWW contaminants (Fig. 4A). High PWW loads have been reported as
315 harmful to the growth of PPB [7,29], PWW dilution being identified as an operational
316 strategy to decrease the turbidity in the cultivation broth, favoring the penetration of the
317 radiation and decreasing the toxic effects of NH_4^+ . A stable biomass concentration of 2.0
318 ± 0.3 g TSS L^{-1} was recorded in the open PBR during stage II, while the increase in
319 temperature and in the evaporation rate entailed an increase in biomass concentration up
320 to 4.9 ± 0.6 g TSS L^{-1} in stage III. Finally, a gradual decrease in biomass concentration in
321 the open PBR to 4.2 ± 0.2 g TSS L^{-1} , 2.4 ± 0.7 g TSS L^{-1} and 2.0 ± 0.4 g TSS L^{-1} was
322 recorded in stages VI, V and VI (Fig. 4A). High TSS-REs were recorded in stage I ($75 \pm$
323 2%) and in the later stages in the open PBR (up 80%) (Fig. 3C). Biomass concentration

324 was stable in the closed PBR, with 2.4 ± 0.3 g TSS L⁻¹ in stage I, and 1.3 ± 0.2 g TSS L⁻¹
325 in stage II-VI, with transient increase in stage V caused by the recirculation of biomass
326 (Fig. 4B). Interestingly, the ratio of culture absorbance at 808 nm and TSS concentration
327 was similar in both PBRs during stages I-V, but significantly higher in the closed PBR
328 when infrared radiation was increased from 100 to 300 W m⁻² (0.013 ± 0.002 in the open
329 PBR to 0.021 ± 0.001 in the closed PBR). TSS-REs in the closed PBR varied from 51 up
330 to 64% (Fig. 3C). The high biomass concentration generated in the open PBR, after stage
331 III did not settle completely, thus increasing the TSS concentrations recorded in the
332 effluent to values similar to the TSS concentrations present in the PWW and also. This
333 fact was also fostered by the low volume of effluent mediated by the high water
334 evaporations prevailing in the latter stage. Interestingly, the lower biomass concentration
335 present in the closed PBR compared to the open PBR was able to removed a similar
336 concentrations of pollutants and generate an effluent with lower TSS. These differences
337 in biomass concentration between both PBRs could be explained by higher water
338 evaporation rate recorded in the open PBR, which indirectly increase the TSS in the PBR.
339 Finally, it should be highlighted that PPB biomass contain high value-added products
340 such single cell protein, pigments, pantothenic acid and coenzyme Q10 [14]. In addition,
341 PPB biomass can be used as animal or fish feed [30] and as a bio-fertilizer, promoting
342 plant growth and boosting the resistance to environmental stresses by accumulation of
343 polyphosphate and synthesizing plant growth-promoting factors [31].

344 <Figure 4>

345 The C, N, H and S content in the PPB biomass averaged $44.3 \pm 1.7\%$, $7.1 \pm 0.8\%$, $6.4 \pm$
346 0.3% and $0.4 \pm 0.3\%$ in the open PBR and $49.8 \pm 0.9\%$, $8.2 \pm 0.4\%$, $7.6 \pm 0.2\%$ and 0.7
347 $\pm 0.2\%$ in the closed PBR, respectively. The PPB biomass composition was similar to the
348 values reported by [32], who recorded a C, N and H content of 52.1%, 10.7% and 8.4%,

349 respectively, in the biomass generated a tubular PBR inoculated with *Rhodospseudomonas*
350 *palustris* strain 42OL.

351 The nitrogen mass balance conducted in the PBRs revealed an overall nitrogen recovery
352 of 67% in the closed PBR, versus 20% in the open PBR. NH₃ stripping was identified as
353 the main nitrogen removal mechanisms in the open PBR, which agreed with the high
354 water evaporation rates recorded in this system.

355

356 The lower investment cost and high nutrient removal capacity constitute the main
357 advantages of open-PBRs [33]. However, the high rates of evaporation and CO₂/NH₃
358 stripping could eventually jeopardize their environmental performance [29,33].
359 Furthermore, culture contamination by other microorganisms is difficult to control in
360 open-PBRs. These limitations are partially mitigated in closed-PBR, where PPB growth
361 and nutrient recovery are also maximized (Table 3). The scalability of the technology is
362 technically feasible in both types of photobioreactors [33]. However, more research is
363 still required to assess microbial competition with other photosynthetic microorganisms
364 in outdoor systems.

365

<Table 3>

366 The evaluation of the scalability of this technology remains the main challenge for the
367 future, with successful case studies such as the work of Lu et al., (2019) where a 240 L
368 reactor was operated with promising resource recovery efficiencies [34]. In addition, the
369 technical and economic viability of the extraction of high added value compounds from
370 PPB in the context of the creation of a circular economy in the water sector remains
371 unexplored.

372

373 **4. Conclusions**

374 This study confirmed the long-term efficiency of PPB-based piggery wastewater
375 treatment. The open PBR always supported higher TOC, TN and TSS removals than the
376 closed PBR, which was mediated by the larger contribution of abiotic mechanisms such
377 as CO₂ and NH₃ stripping. The decrease in PWW load did not entail an enhancement in
378 process performance in both PBRs, while the increase in the illuminated area to volume
379 ratio induced higher TOC and TN removals. Biomass settling and recirculation resulted
380 in enhanced nitrogen removals. Finally, the increase in infrared radiation from 100 to 300
381 W m⁻² favored PPB growth. The high water evaporation losses in the open PBR resulted
382 in a significant deterioration of the effluent quality as a result of pollutant pre-
383 concentration. PWW dilution and operation with high illuminated area were key
384 parameters that favored PPB growth in the closed PBR. In addition, this type of PBR
385 configuration prevents high water evaporations and favors the dominance of PPB.

386

387 **Acknowledgements**

388 The financial support from the Regional Government of Castilla y León, the EU-FEDER
389 programme (CLU 2017-09 and UIC 071), CONICYT (PFCHA/DOCTORADO BECAS
390 CHILE/2017 – 72180211) and CONACYT-SENER program (Ref: 438909) is gratefully
391 acknowledged. The authors also thank Enrique Marcos, Araceli Crespo and Beatriz
392 Muñoz for their technical assistance.

393

394 **Supplementary Materials:** Figure S1: Time course of the temperatures (A), dissolved
395 oxygen concentration (B), pH (C) and IR radiation (D) during PWW biodegradation by
396 PPB.

397

398

399 **References**

- 400 [1] Y. Yang, E. Lin, S. Sun, X. Tao, L. Zhong, K. Hu, Piggery wastewater treatment
401 by *Acinetobacter* sp. TX5 immobilized with spent mushroom substrate in a fixed-
402 bed reactor, *Sci. Total Environ.* 644 (2018) 1460–1468.
403 <https://doi.org/10.1016/J.SCITOTENV.2018.07.076>.
- 404 [2] G. Chen, J. Huang, X. Tian, Q. Chu, Y. Zhao, H. Zhao, Effects of influent loads
405 on performance and microbial community dynamics of aerobic granular sludge
406 treating piggery wastewater, *J. Chem. Technol. Biotechnol.* 93 (2018) 1443–
407 1452. <https://doi.org/10.1002/jctb.5512>.
- 408 [3] I. de Godos, S. Blanco, P.A. García-Encina, E. Becares, R. Muñoz, Long-term
409 operation of high rate algal ponds for the bioremediation of piggery wastewaters
410 at high loading rates, *Bioresour. Technol.* 100 (2009) 4332–4339.
411 <https://doi.org/10.1016/J.BIORTECH.2009.04.016>.
- 412 [4] M.J. Luján-Facundo, M.I. Iborra-Clar, J.A. Mendoza-Roca, M. Also-Jesús,
413 Alternatives for the management of pig slurry: Phosphorous recovery and biogas
414 generation, *J. Water Process Eng.* 30 (2019) 100473.
415 <https://doi.org/10.1016/j.jwpe.2017.08.011>.
- 416 [5] I. de Godos, V.A. Vargas, S. Blanco, M.C.G. González, R. Soto, P.A. García-
417 Encina, E. Becares, R. Muñoz, A comparative evaluation of microalgae for the
418 degradation of piggery wastewater under photosynthetic oxygenation, *Bioresour.*
419 *Technol.* 101 (2010) 5150–5158.
420 <https://doi.org/10.1016/J.BIORTECH.2010.02.010>.
- 421 [6] D. García, I. de Godos, C. Domínguez, S. Turiel, S. Bolado, R. Muñoz, A
422 systematic comparison of the potential of microalgae-bacteria and purple
423 phototrophic bacteria consortia for the treatment of piggery wastewater,

- 424 Bioresour. Technol. 276 (2019) 18–27.
425 <https://doi.org/10.1016/J.BIORTECH.2018.12.095>.
- 426 [7] D. Marín, E. Posadas, D. García, D. Puyol, R. Lebrero, R. Muñoz, Assessing the
427 potential of purple phototrophic bacteria for the simultaneous treatment of
428 piggery wastewater and upgrading of biogas, *Bioresour. Technol.* 281 (2019) 10–
429 17. <https://doi.org/10.1016/J.BIORTECH.2019.02.073>.
- 430 [8] L. de S. Leite, M.T. Hoffmann, L.A. Daniel, Microalgae cultivation for
431 municipal and piggery wastewater treatment in Brazil, *J. Water Process Eng.* 31
432 (2019) 100821. <https://doi.org/10.1016/j.jwpe.2019.100821>.
- 433 [9] L. de S. Leite, M.T. Hoffmann, L.A. Daniel, Coagulation and dissolved air
434 flotation as a harvesting method for microalgae cultivated in wastewater, *J. Water
435 Process Eng.* 32 (2019) 100947. <https://doi.org/10.1016/j.jwpe.2019.100947>.
- 436 [10] T. Hülsen, K. Hsieh, S. Tait, E.M. Barry, D. Puyol, D.J. Batstone, White and
437 infrared light continuous photobioreactors for resource recovery from poultry
438 processing wastewater – A comparison, *Water Res.* 144 (2018) 665–676.
439 <https://doi.org/10.1016/J.WATRES.2018.07.040>.
- 440 [11] A. Talaiekhosani, S. Rezania, Application of photosynthetic bacteria for removal
441 of heavy metals, macro-pollutants and dye from wastewater: A review, *J. Water
442 Process Eng.* 19 (2017) 312–321. <https://doi.org/10.1016/j.jwpe.2017.09.004>.
- 443 [12] T. Hülsen, D.J. Batstone, J. Keller, Phototrophic bacteria for nutrient recovery
444 from domestic wastewater, *Water Res.* 50 (2014) 18–26.
445 <https://doi.org/10.1016/J.WATRES.2013.10.051>.
- 446 [13] T. Hülsen, E.M. Barry, Y. Lu, D. Puyol, D.J. Batstone, Low temperature
447 treatment of domestic wastewater by purple phototrophic bacteria: Performance,
448 activity, and community., *Water Res.* 100 (2016) 537–545.

- 449 <https://doi.org/10.1016/J.WATRES.2016.05.054>.
- 450 [14] H. Lu, G. Zhang, Z. Zheng, F. Meng, T. Du, S. He, Bio-conversion of
451 photosynthetic bacteria from non-toxic wastewater to realize wastewater
452 treatment and bioresource recovery: A review, *Bioresour. Technol.* 278 (2019)
453 383–399. <https://doi.org/10.1016/J.BIORTECH.2019.01.070>.
- 454 [15] H. Lu, G. Zhang, S. Dong, Quantitative study of PNSB energy metabolism in
455 degrading pollutants under weak light-micro oxygen condition, *Bioresour.*
456 *Technol.* 102 (2011) 4968–4973.
457 <https://doi.org/10.1016/J.BIORTECH.2011.01.027>.
- 458 [16] E. Siefert, R.L. Irgens, N. Pfennig, Phototrophic purple and green bacteria in a
459 sewage treatment plant., *Appl. Environ. Microbiol.* 35 (1978) 38–44.
460 <http://www.ncbi.nlm.nih.gov/pubmed/623470> (accessed October 18, 2019).
- 461 [17] F.W. Larimer, P. Chain, L. Hauser, J. Lamerdin, S. Malfatti, L. Do, M.L. Land,
462 D.A. Pelletier, J.T. Beatty, A.S. Lang, F.R. Tabita, J.L. Gibson, T.E. Hanson, C.
463 Bobst, J.L.T. y Torres, C. Peres, F.H. Harrison, J. Gibson, C.S. Harwood,
464 Complete genome sequence of the metabolically versatile photosynthetic
465 bacterium *Rhodospseudomonas palustris*, *Nat. Biotechnol.* 22 (2004) 55–61.
466 <https://doi.org/10.1038/nbt923>.
- 467 [18] K. Cao, R. Zhi, G. Zhang, Photosynthetic bacteria wastewater treatment with the
468 production of value-added products: A review, *Bioresour. Technol.* (2019)
469 122648. <https://doi.org/10.1016/J.BIORTECH.2019.122648>.
- 470 [19] Q. Zhou, P. Zhang, G. Zhang, M. Peng, Biomass and pigments production in
471 photosynthetic bacteria wastewater treatment: Effects of photoperiod, *Bioresour.*
472 *Technol.* 190 (2015) 196–200.
473 <https://doi.org/10.1016/J.BIORTECH.2015.04.092>.

- 474 [20] T. Hülsen, E.M. Barry, Y. Lu, D. Puyol, J. Keller, D.J. Batstone, Domestic
475 wastewater treatment with purple phototrophic bacteria using a novel continuous
476 photo anaerobic membrane bioreactor, *Water Res.* 100 (2016) 486–495.
477 <https://doi.org/10.1016/J.WATRES.2016.04.061>.
- 478 [21] S. Chitapornpan, C. Chiemchaisri, W. Chiemchaisri, R. Honda, K. Yamamoto,
479 Organic carbon recovery and photosynthetic bacteria population in an anaerobic
480 membrane photo-bioreactor treating food processing wastewater, *Bioresour.*
481 *Technol.* 141 (2013) 65–74. <https://doi.org/10.1016/j.biortech.2013.02.048>.
- 482 [22] J. Kaewsuk, W. Thorasampan, M. Thanuttamavong, G.T. Seo, Kinetic
483 development and evaluation of membrane sequencing batch reactor (MSBR) with
484 mixed cultures photosynthetic bacteria for dairy wastewater treatment, *J.*
485 *Environ. Manage.* 91 (2010) 1161–1168.
486 <https://doi.org/10.1016/j.jenvman.2010.01.012>.
- 487 [23] L. Goswami, R. Vinoth Kumar, S.N. Borah, N. Arul Manikandan, K.
488 Pakshirajan, G. Pugazhenthii, Membrane bioreactor and integrated membrane
489 bioreactor systems for micropollutant removal from wastewater: A review, *J.*
490 *Water Process Eng.* 26 (2018) 314–328.
491 <https://doi.org/10.1016/j.jwpe.2018.10.024>.
- 492 [24] Z. Zhong, X. Wu, L. Gao, X. Lu, B. Zhang, Efficient and microbial communities
493 for pollutant removal in a distributed-inflow biological reactor (DBR) for treating
494 piggery wastewater, *RSC Adv.* 6 (2016) 95987–95998.
495 <https://doi.org/10.1039/c6ra20777d>.
- 496 [25] APHA, *Standard Methods for the Examination of Water and Wastewater*, 21st
497 ed. American Public Health Association, Washington, DC, USA., (2005).
- 498 [26] C.B. van Niel, *The culture, general physiology, morphology, and classification of*

499 the non-sulfur purple and brown bacteria, *Bacteriol. Rev.* 8 (1944) 1–118.
500 <http://www.ncbi.nlm.nih.gov/pubmed/16350090> (accessed October 3, 2019).

501 [27] W.Y. Cheah, T.C. Ling, P.L. Show, J.C. Juan, J.S. Chang, D.J. Lee, Cultivation
502 in wastewaters for energy: A microalgae platform, *Appl. Energy.* 179 (2016)
503 609–625. <https://doi.org/10.1016/j.apenergy.2016.07.015>.

504 [28] F. Meng, A. Yang, G. Zhang, H. Wang, Effects of dissolved oxygen
505 concentration on photosynthetic bacteria wastewater treatment: Pollutants
506 removal, cell growth and pigments production, *Bioresour. Technol.* 241 (2017)
507 993–997. <https://doi.org/10.1016/j.biortech.2017.05.183>.

508 [29] C.A. Sepúlveda-Muñoz, I. de Godos, D. Puyol, R. Muñoz, A systematic
509 optimization of piggery wastewater treatment with purple phototrophic bacteria,
510 *Chemosphere.* 253 (2020) 126621.
511 <https://doi.org/10.1016/j.chemosphere.2020.126621>.

512 [30] M. Kobayashi, Y.T. Tchan, Treatment of industrial waste solutions and
513 production of useful by-products using a photosynthetic bacterial method, *Water*
514 *Res.* 7 (1973) 1219–1224. [https://doi.org/10.1016/0043-1354\(73\)90075-4](https://doi.org/10.1016/0043-1354(73)90075-4).

515 [31] M. Sakarika, J. Spanoghe, Y. Sui, E. Wambacq, O. Grunert, G. Haesaert, M.
516 Spiller, S.E. Vlaeminck, Purple non-sulphur bacteria and plant production:
517 benefits for fertilization, stress resistance and the environment, *Microb.*
518 *Biotechnol.* (2019) 1751-7915.13474. <https://doi.org/10.1111/1751-7915.13474>.

519 [32] P. Carozzi, B. Pushparaj, A. Degl’Innocenti, A. Capperucci, Growth
520 characteristics of *Rhodospseudomonas palustris* cultured outdoors, in an
521 underwater tubular photobioreactor, and investigation on photosynthetic
522 efficiency, *Appl. Microbiol. Biotechnol.* 73 (2006) 789–795.
523 <https://doi.org/10.1007/s00253-006-0550-z>.

524 [33] L. Christenson, R. Sims, Production and harvesting of microalgae for wastewater
525 treatment, biofuels, and bioproducts, *Biotechnol. Adv.* 29 (2011) 686–702.
526 <https://doi.org/10.1016/j.biotechadv.2011.05.015>.

527 [34] H. Lu, M. Peng, G. Zhang, B. Li, Y. Li, Brewery wastewater treatment and
528 resource recovery through long term continuous-mode operation in pilot
529 photosynthetic bacteria-membrane bioreactor, *Sci. Total Environ.* 646 (2019)
530 196–205. <https://doi.org/10.1016/j.scitotenv.2018.07.268>.

531 [35] A.P. Carvalho, L.A. Meireles, F.X. Malcata, Microalgal Reactors: A Review of
532 Enclosed System Designs and Performances, *Biotechnol. Prog.* 22 (2006) 1490–
533 1506. <https://doi.org/10.1021/bp060065r>.

534 [36] O. Pulz, Photobioreactors: Production systems for phototrophic microorganisms,
535 *Appl. Microbiol. Biotechnol.* 57 (2001) 287–293.
536 <https://doi.org/10.1007/s002530100702>.

537

538

539

540

541

542

543

544

545

546

547 **List of tables**

548

549 **Table 1.** Summary of photobioreactors operational period and conditions. Description of
550 the PWW dilution, culture depth, temperature control, biomass recirculation and infrared
551 radiation intensity.

552

553 **Table 2.** Summary of PWW composition, environmental variables, cultivation broth and
554 effluent characteristics in the open and closed photobioreactors during steady state along
555 the different operational stages (values represent average values \pm standard deviation).

556

557 **Table 3.** Advantages and limitations of open and closed photobioreactors. Comparative
558 qualitative assessment of the economic and environmental performance of PPB-based
559 open and closed photobioreactors.

560

561

562

563

564

565

566

567

568 **List of figures**

569

570 **Figure 1.** Schematic diagram of the PPB-based open and closed photobioreactors. The
571 system is composed of a feeding tank, an open and closed PBR, settlers and effluent tanks.

572

573 **Figure 2.** Time course of the concentration of TOC (A) and TN (B) in the raw PWW and
574 effluent from the open and closed PBR. This graph shows the long-term dynamics of the
575 main pollutants degraded by PPB.

576

577 **Figure 3.** Removal efficiencies of TOC (A), TN (B) and TSS (C) in the open and closed
578 photobioreactors during steady state in the different operational stages of piggery
579 wastewater treatment by PPB. Removal efficiencies were estimated based on the
580 concentrations and flow rates at the inlet and outlet of the PBRs.

581

582 **Figure 4.** Time course of TSS concentration in open (A) and closed (B) photobioreactors
583 during the treatment of PWW by PPB. The concentration of solids in the influent, biomass
584 in the culture broth and effluent are here depicted.

585

586

587

588

589

590 **Table 1.**

Stage	Operational days	Dilution of PWW	Depth of culture (cm) / area to volume ratio (cm² L⁻¹)	Temperature control	Recirculation	Infrared radiation (W m⁻²)
I	101	4	15 / 66.7	No	No	100
II	67	8	15 / 66.7	No	No	100
III	70	8	7.5 / 133	No	No	100
IV	63	8	7.5 / 133	Yes	No	100
V	108	8	7.5 / 133	Yes	Yes	100
VI	53	8	7.5 / 133	Yes	Yes	300

591

592

593

594

595

596 **Table 2.**

Parameters	PWW*	Stage I		Stage II		Stage III		Stage IV		Stage V		Stage VI	
		Open	Closed										
Temperature (°C)	-	31.7±1.4	35.3±2.5	30.7±1.2	32.7±1.4	33.2±1.2	36.4±2.5	30.5±1.0	34.5±1.7	32.0±1.3	36.3±1.8	34.4±0.06	39.9±1.6
pH	7.8±0.3	8.7±0.2	8.1±0.3	8.7±0.1	8.3±0.2	8.8±0.1	8.4±0.1	8.8±0.1	8.4±0.1	8.8±0.1	8.2±0.1	8.7±0.1	8.5±0.1
Radiation IR (W m ⁻²)	-	97±7		97±4		93±4		99±7		101±4		293±7	
Evaporation (%)	-	58±1	10±2	58±1	10±2	97±3	30±18	84±15	14±6	89±6	17±7	99±3	11±5
TOC (g L ⁻¹)	1.18±0.15	0.89±0.06	0.84±0.06	0.35±0.05	0.29±0.04	0.34±0.03	0.27±0.02	0.66±0.07	0.17±0.03	0.42±0.04	0.15±0.03	0.50±0.05	0.14±0.03
IC (g L ⁻¹)	0.13±0.04	0.54±0.03	0.67±0.04	0.32±0.01	0.39±0.01	0.25±0.08	0.29±0.04	0.43±0.04	0.21±0.03	0.39±0.01	0.16±0.02	0.41±0.06	0.16±0.03
TN (g L ⁻¹)	0.38±0.05	0.50±0.03	0.81±0.03	0.27±0.01	0.36±0.01	0.12±0.03	0.27±0.03	0.12±0.02	0.22±0.05	0.08±0.01	0.10±0.03	0.09±0.02	0.10±0.0
NH₄⁺ (g L ⁻¹)	0.40±0.12	0.43±0.05	0.80±0.05	0.24±0.02	0.37±0.03	0.04±0.05	0.17±0.07	0.00±0.00	0.17±0.02	-	-	0.02±0.01	0.08±0.02
TSS PBR (g L ⁻¹)		3.80±0.35	2.40±0.30	1.97±0.18	1.44±0.09	4.90±0.65	1.46±0.22	4.19±0.20	1.26±0.09	2.37±0.65	1.36±0.41	1.97±0.44	1.03±0.11
TSS Effluent (g L ⁻¹)	1.31±0.28	1.63±0.11	1.45±0.18	0.81±0.09	0.67±0.06	0.56±0.18	0.72±0.13	1.59±0.23	0.83±0.22	0.93±0.11	0.51±0.05	0.92±0.10	0.44±0.08

597 - Not applicable.

598 * 8 fold diluted PWW (in tap water).

599 TOC, IC, TN, NH₄⁺ correspond to the concentration in the effluent of the photobioreactors.

600

601 **Table 3.**

	Open-PBR	Closed-PBR	Reference
Nutrient removal	High	High	[29]
Nutrient recovery in biomass	Low	High	[29]
Biomass growth	Medium	High	[29]
Culture contamination	High	Low	[27,33,35,36]
Evaporation rate	High	Low	[27,33,35,36]
Culture control	Low	High	[33,35,36]
Environmental impact*	High	Low	[23,29,36]
Investment costs	Low	High	[33,35]
Scalability	High	Medium	[29,33]

602 * Atmospheric pollution by stripping CO₂ and NH₃.

603

604

605

606

607

608

609

610

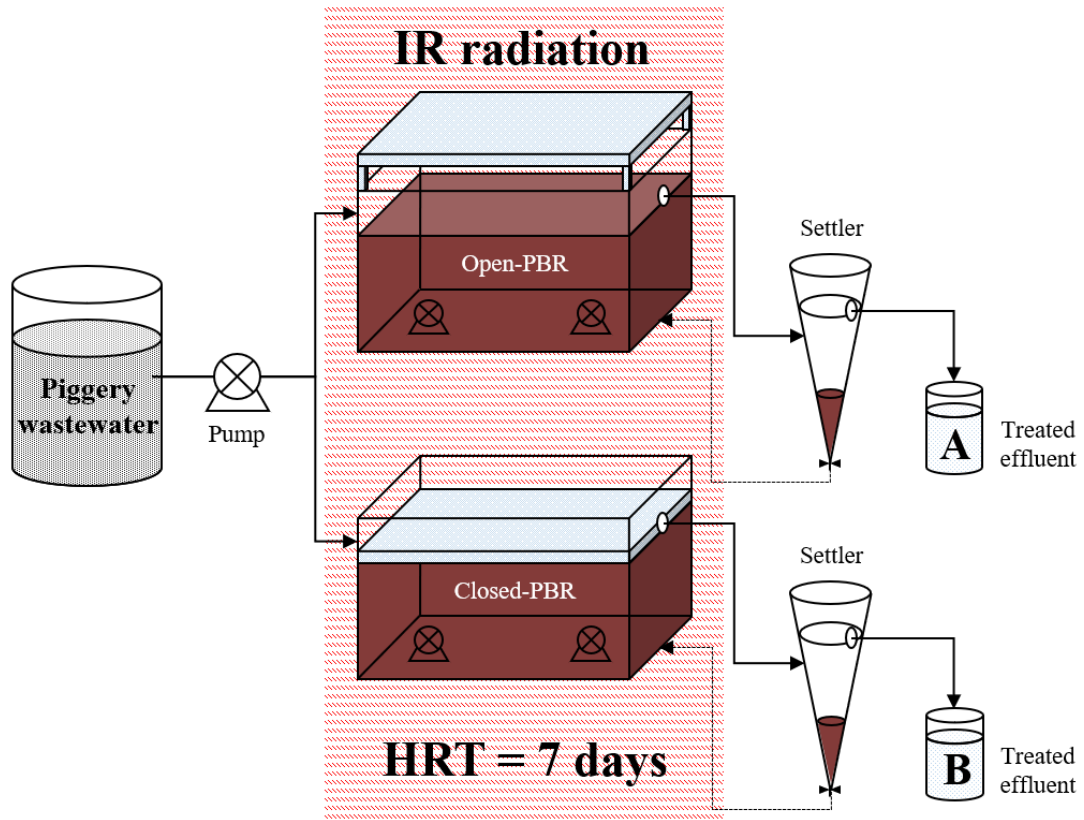
611

612

613

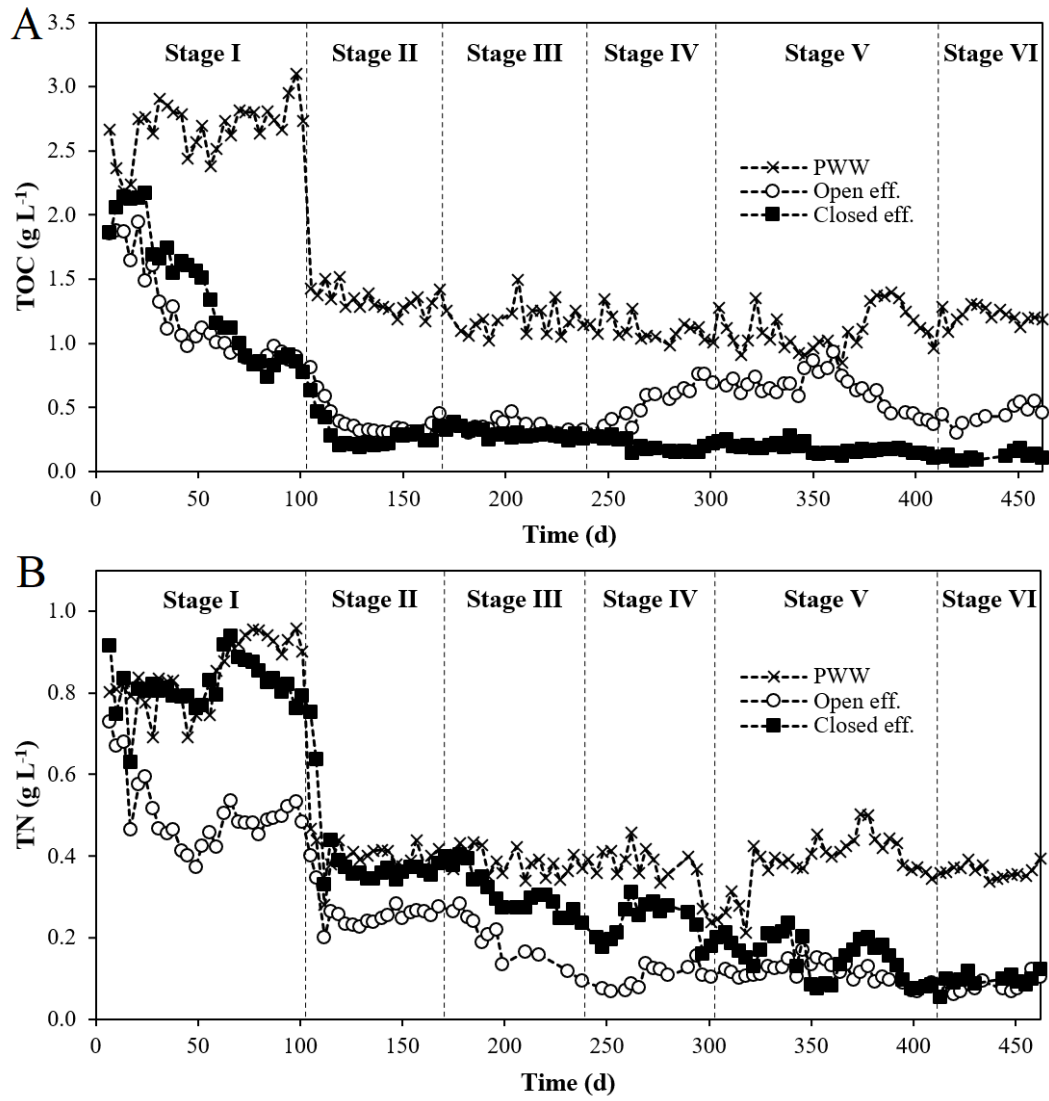
614

615 **Figure 1.**



616
617
618
619
620
621
622
623
624
625
626

627 **Figure 2.**



628

629

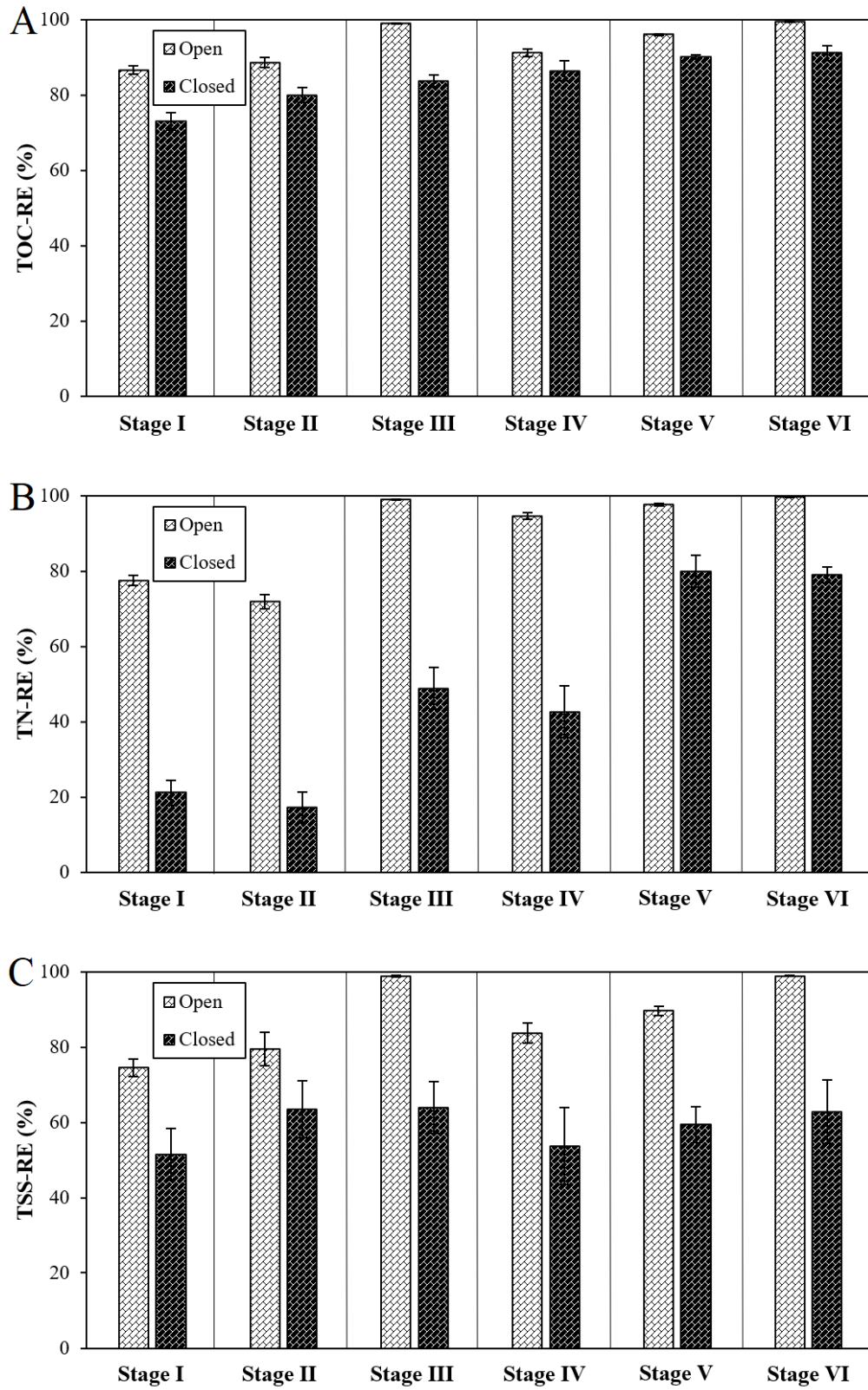
630

631

632

633

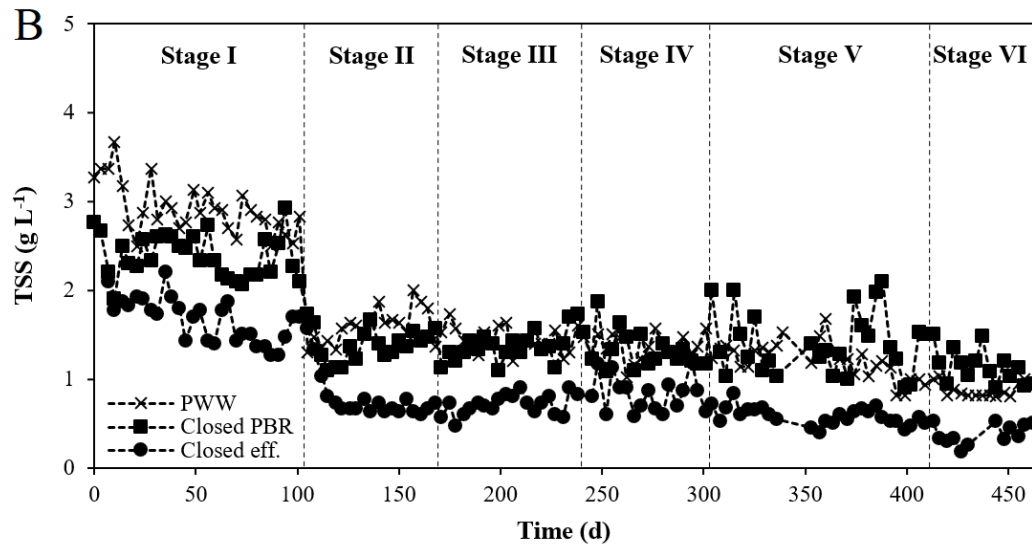
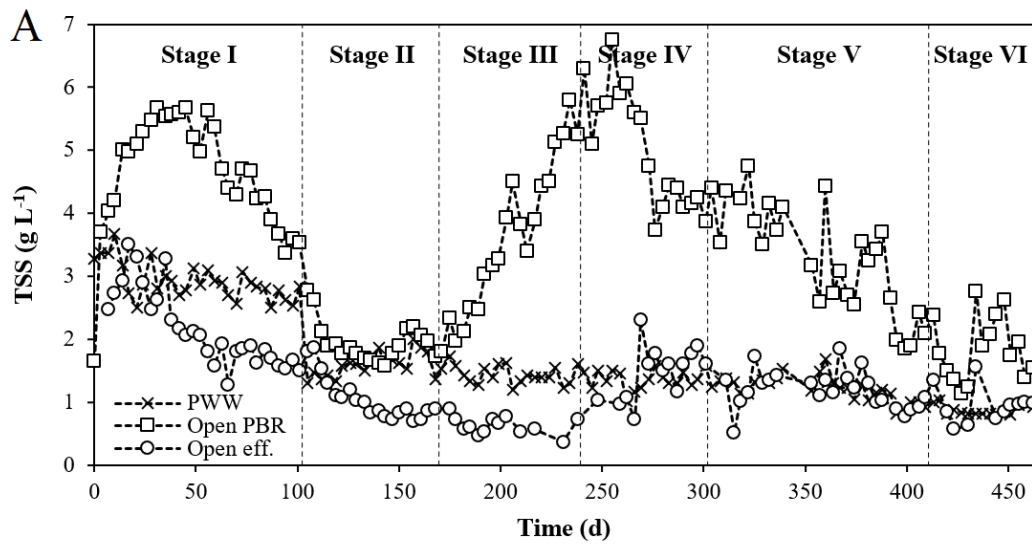
634



636

637

638 **Figure 4.**



639

640

641

642

643

644

645